Analysis of a semi-Lagrangian numerical method in a cell dwarfism model

L. M. Abia[a], O. Angulo[b], J.C. López-Marcos[a] and M.A. López-Marcos[a]

[a] Departamento de Matemática Aplicada & IMUVA, Facultad de Ciencias, Valladolid, Spain
[b] Departamento de Matemática Aplicada & IMUVA, ETS de Ingenieros de Telecomunicación, Valladolid, Spain

ARTICLE HISTORY
Compiled August 30, 2022

ABSTRACT
In this work, we introduce a new semi-Lagrangian numerical method proposed to solve a cell population balance model which describes cell dwarfism, by allowing cell division at any size. We analyze its convergence and derive an optimal rate. Numerical experiments are reported to demonstrate the predicted accuracy of the scheme. Finally, the good behavior of the numerical method is exhibited in stressed conditions that can provoke lack of smoothness and simulations are included to show how the increase in the division rate of small size-cells promotes dynamics in which nonfunctional dwarf cells are saturating the total cell population.

KEYWORDS
Cell population balance model; dwarfism; semi-Lagrangian method; convergence analysis

1. Introduction

In this work, we analyze a numerical method proposed to obtain the solution of a specific cell population balance model (CPBM) in which cells of any size may divide. This is an abnormal model in the sense that we do not assume a minimal positive cell size for cellular division to take place. The model is based upon the one developed by Diekmann *et al.* [6], and analyzed first by Howard [10].

We consider an unlimited environment in which all possible nonlinear mechanisms are ignored, where cells are distinguished by their individual size, represented by x. Cells size grows exponentially, $x'(t) = x(t)$, as in a Petri dish experiment, where t represents time. The size-distribution of the cell population at time t is given by a function $u(x,t)$. As time evolves, the following processes are also relevant in the model: cells die with a death rate $\mu(x)$ and a mother cell splits into two equal daughter cells with a division rate $b(x)$; both vital functions depend on the cell size. We deviate from the usual cell population balance model by incorporating a source term to take into account the immigration of new cells from a regulatory source, in which a renewal of the cell population occurs at a rate $\nu(x)$ depending upon cell size. An example for this kind of regulation is given by the blood production system, which needs to replace the red blood cells daily in order to sustain a viable population. In case of a closed system,

Email: lmabia@uva.es (L. M. Abia), oscar.angulo@uva.es (O. Angulo), lopezmar@mac.uva.es (J.C. López-Marcos), malm@mac.uva.es (M.A. López-Marcos)

as in a Petri dish, we have to consider $\nu(x) \equiv 0$. The model is given by the following initial value problem, which consists in a partial differential equation that represents the balance of the size structured cell population and an initial condition,

$$u_t(x,t) + (x\,u(x,t))_x = (\nu(x) - \mu(x) - b(x))\,u(x,t) + 4\,b(2\,x)\,u(2\,x,t), \quad 0 < x < 1,\ t > 0, \tag{1.1}$$

$$u(x,0) = \varphi(x), \quad 0 \le x \le 1, \tag{1.2}$$

where we assume that the death rate $\mu(x)$, and the division rate $b(x)$ are both positive, and $\nu(x)$ is nonnegative. Its dynamics are completely determined once we know the vital functions (μ, b and ν) and the initial state of the population density. We want to point out that a proper combination of growth, division and mortality rates would introduce a natural maximum cell size [1]. Otherwise we could fix it as one (normalized) and we would consider that larger cells may only grow and die.

From a theoretical point of view, mathematical treatment of lineal CPBMs has been developed since the early eighties [6, 8, 9], where the study of the well-posedness, the convergence towards an *asymptotically stable size distribution* and the stability analysis were carried out. In the case of nonlinear models, the theoretical properties of existence and uniqueness of solutions have been addressed in [9]. These models assume the existence of a minimal cell size $a > 0$ for cellular division to take place, which generates a minimal cell size $a/2$.

In the particular model we present, an abnormal behavior occurs: cells of any size may divide. Consequently, the minimal cell size is set to $a = 0$. The idea of a cell with size zero is biologically unrealistic, although it could be considered as a limit value to describe an abnormality in the cellular division process: the accumulation of cells of various sizes including a population of non-functional "dwarf" cells. The presence of such "dwarf" cells is observed in the hereditary blood disorder known as α-thalassemia which is associated with sickle cell anemia. It has the effect of greatly reducing the mean corpuscle volume of red blood cells, what is known as microcytosis [7, 13]. Some theoretical properties of this particular model (1.1)-(1.2) were developed by Howard [10], where the existence and uniqueness of generalized solutions and their stability and unstability was addressed. In particular, a representation of the generalized theoretical solution of (1.1)-(1.2) was given by

$$u(x,t) = \sum_{n=0}^{\infty} K_n(x,t)\,\varphi(2^n\,x\,e^{-t}), \tag{1.3}$$

in which the multiplicative factors $K_n(x,t)$ were computed successively as

$$K_0(x,t) := \exp\left(\int_0^t \mu^*(x\,e^{-r})\,dr\right),$$

$$K_n(x,t) := 4^n \int_0^t \int_0^{s_n} \cdots \int_0^{s_2} \exp\left(\int_0^{t-s_n} \mu^*(x\,e^{-r})\,dr + \int_{t-s_n}^{t-s_{n-1}} \mu^*(2\,x\,e^{-r})\,dr \right.$$
$$\left. + \cdots + \int_{t-s_1}^{t} \mu^*(2^n\,x\,e^{-r})\,dr\right) b(2\,x\,e^{-(t-s_n)}) \cdots b(2^n\,x\,e^{-(t-s_1)})\,ds_1 \ldots ds_{n-1} ds_n,$$

$n = 1, 2, \ldots$. Here $\mu^*(x) = 1 + \mu(x) + b(x) - \nu(x)$.

It is not an easy task to obtain an explicit formula for $u(x,t)$ even in the case of constant death, division and migration rates. Also, data functions properties were proposed to arrive to the topological transitivity of the different cellular generations. Such an issue has been subsequently refined (see [11, 12] and references therein). The theoretical representation (1.3) for the solution, although explicit, does not provide a method to compute the solution for general function data $\mu(x)$, $b(x)$ and $\nu(x)$.

However, the knowledge of their qualitative or quantitative behavior in a more tangible way is sometimes necessary. Therefore, numerical methods provide a valuable tool to obtain such quantitative information. Different techniques have been used for both symmetric and asymmetric division rates (see [1, 4, 5] and the references therein). However, in general, they are proposed for the solution of models with a positive minimal cell division size, and it is very important to design numerical schemes specially adapted to the characteristics of this particular CPBM. We proposed two first-order numerical schemes in [2] based on classical techniques. Here, we present and analyze a new first-order method based on the discretization of the solution along the characteristic curves, but now on a fixed grid: the so-called semi-Lagrangian technique. It is specially adapted to obtain the solution to the problem (1.1)-(1.2) and combines the advantages of finite difference and characteristics schemes. This procedure has been previously considered for a cell model with a positive minimal cell size [3].

We want to point out that the exponential growth introduces a characteristic curve at the minimum size. As a consequence, there is no recruitment from the boundary, which represents the unavailability of a left boundary condition in opposition to what is usual in this kind of hyperbolic problems.

The paper is organized as follows. Section 2 is devoted to the description of the proposed numerical method. In Section 3, we analyze the convergence of the numerical scheme, and in Section 4 we carry out a representative numerical simulation, including stressed conditions that can provoke lack of smoothness and experiments to show the proportion of nonfunctional dwarf cells in the total cell population.

2. Numerical Method

The main objective of this work consists in integrating numerically the problem (1.1)-(1.2) on a fixed time interval $[0, T]$. This model presents several special features we must avoid in the proposal of a new numerical method. First, hyperbolic evolutionary problems are usually described with a left or right hand boundary (depending on the flow direction) when a bounded domain is declared. However, in this case, the left boundary condition is a characteristic curve of the problem and, therefore, there is not a useful definition of the solution on this boundary that we must avoid numerically. Second, in general, the combination of the vital functions (growth, mortality and division rates) do not carry out to the existence of a natural maximum cell size. Thus, cells grow further than the maximum division size ($x = 1$) and beyond this value they only grow and die. This question makes the solution of the problem not to be regular enough to employ high order methods. In the following we describe a numerical scheme of first order specially adapted to the model that circumvents these peculiarities.

The method we present is based on the integration of the problem along the characteristic curves, thus we transform the problem. First, we rewrite (1.1) as

$$u_t(x,t) + x\, u_x(x,t) \quad = \quad -\mu^*(x)\, u(x,t) + 4\, b(2\,x)\, u(2\,x,t), \tag{2.1}$$

$0 < x < 1$, $t > 0$. Now, we denote by $x(t; t^*, x_*) = x_* \exp(t - t^*)$, the characteristic curve of the equation (2.1) (and (1.1)) which takes the value x_* at time t^*, and we define $w(t; t^*, x_*) = u(x(t; t^*, x_*), t)$, $t \geq t^*$. It satisfies

$$\begin{cases} \dfrac{d}{dt} w(t; t^*, x_*) = -\mu^*(x(t; t^*, x_*))\, w(t; t^*, x_*) + 4\, b(2\, x(t; t^*, x_*))\, u(2\, x(t; t^*, x_*), t), \\ \qquad\qquad\qquad\qquad\qquad\qquad\qquad\qquad\qquad\qquad\qquad\qquad t > t^*, \\ w(t^*; t^*, x_*) = u(x_*, t^*). \end{cases} \tag{2.2}$$

The solution to (2.2) can be written as (see [4])

$$u(x(t; t^*, x_*), t) = u(x_*, t^*) \exp\left\{ -\int_{t^*}^{t} \mu^*\left(x(\tau; t^*, x_*)\right)\, d\tau \right\}$$

$$+ 4 \int_{t^*}^{t} \exp\left\{ -\int_{\tau}^{t} \mu^*\left(x(s; t^*, x_*)\right) ds \right\} b(2\, x(\tau; t^*, x_*))\, u(2\, x(\tau; t^*, x_*), \tau) d\tau, t \geq t^*. \tag{2.3}$$

We will employ this formula in the design of the numerical method.

In the following we detail the numerical procedure. First, we introduce a uniform grid on the size domain. Let J be a positive integer, we define the discretization parameter in size, $h = 1/(2\,J)$, and the grid points as $X_j = j\, h$, $0 \leq j \leq 2\, J$. Hence, $X_J = 1/2$ and $X_{2\,J} = 1$, therefore the possible discontinuity point and the normalized maximum size are on the grid. This is a particularity of the scheme. It employs a uniform grid on the size interval, as a finite difference method does, and avoids the accumulation of the grid nodes which usually affects common methods that employ the integration along the characteristics.

Next, we introduce the discretization parameter in time $k > 0$, define $N = \lfloor T/k \rfloor$ and the discrete time levels $t^n = n\, k$, $0 \leq n \leq N$. From now on, we refer to the grid point X_j with a subscript j, and to the time level t^n with a superscript n, and we denote $u_j^n = u(X_j, t^n)$, as the values of the solution restricted to the grid points, and U_j^n will be a numerical approximation to u_j^n, $0 < j \leq 2\, J$, $0 \leq n \leq N$. We also employ the vectorial notation $\mathbf{U}^n = (U_1^n, U_2^n, \ldots, U_{2\,J}^n)$, $0 \leq n \leq N$.

Now, we propose a one-step method based on the discretization of (2.3) that involves points in the same characteristic curve. Therefore, first we have to compute an auxiliary grid, with points that are on the same characteristic curve as the corresponding values of the uniform grid, $Y_j = X_j \exp(-k)$, $1 \leq j \leq 2\, J$. It represents the grid at the previous time level. The approximation to the solution at this new grid points, $u(Y_j, t^n)$, will be denoted as $\bar{U}_j^n$, $1 \leq j \leq 2\, J$, $1 \leq n \leq N$. Finally, as we discussed above, there is no left boundary condition, therefore we do not define the value of U_0^n, $1 \leq n \leq N$.

Thus, once we introduce $\mathbf{U}^0$, an approximation to the discrete restriction to the grid of the initial condition, the general step is obtained by means of the following first-order discretization of (2.3), for $0 \leq n \leq N - 1$,

$$U_j^{n+1} = \bar{U}_j^n \exp\left\{-k\, \mu_j^*\right\} + 4\, k\, b_{2\,j}\, U_{2\,j}^{n+1}, \quad 1 \leq j \leq J, \tag{2.4}$$

$$U_j^{n+1} = \bar{U}_j^n \exp\left\{-k\, \mu_j^*\right\}, \quad J + 1 \leq j \leq 2\, J, \tag{2.5}$$

where $\mu_j^* = \mu^*(X_j)$, $b_j = b(X_j)$, $1 \leq j \leq 2\, J$. The numerical method is completely

defined once $\bar{U}_j^n$, $1 < j \leq 2\,J$, $1 \leq n \leq N$, is computed. We define $\bar{U}_j^n = U_1^n$, when $Y_j \in (0, X_1]$, and

$$\bar{U}_j^n = U_{j-r_j}^n + (U_{j-r_j+1}^n - U_{j-r_j}^n)\,\frac{Y_j - X_{j-r_j}}{h}, \tag{2.6}$$

with $r_j \in \mathbb{N}$, such that $X_{j-r_j} \leq Y_j < X_{j-r_j+1}$, $1 \leq j \leq 2\,J$. We note that, assuming the time discretization parameter $k < \ln(2)$, we assure that $Y_j > X_1$ and, therefore, the interpolatory formula (2.6) is applicable for $2 \leq j \leq 2\,J$. We have to notice that: first, we allow Y_j to move backwards without constraining it to belong to the interval $[X_{j-1}, X_j]$. Second, with respect to the size grid given by Y_j, $1 \leq j \leq 2\,J$, the integer shift r_j that localizes each Y_j within the corresponding interval $[X_{j-r_j}, X_{j-r_j+1}]$, and the coefficients of the linear interpolation, are computed only once. The unique exception to this computation is when $\bar{U}_1^n$ must be approximated by the constant value U_1^n, because we do not have information on the left boundary $x = 0$.

This numerical procedure seems to be implicit. However, if we compute the approximations at the new time level t^{n+1} backwards it turns out to be explicit. We compute first U_j^{n+1} from $J+1$ to $2\,J$ using (2.5); next, backwards, U_j^{n+1} from J to 1 by means of (2.4).

3. Convergence Analysis

In this section, the convergence analysis of the scheme is performed. The linearity of the model allows us to present it in a matrix form. The study of the amplification due to the matrix (stability) and the consistency carry out the convergence of the method.

The description of the numerical scheme can be made in matrix form as

$$(\mathcal{I} - \mathcal{B}(k))\,\mathbf{U}^{n+1} = \mathcal{D}(k)\,\mathbf{U}^n,$$

where $\mathcal{I}$ is the identity matrix in $\mathcal{M}_{(2\,J)\times(2\,J)}(\mathbb{R})$, $\mathcal{B}(k) = (b_{i,j}(k))_{i,j=1}^{2\,J}$ and $\mathcal{D}(k) = (d_{i,j}(k))_{i,j=1}^{2\,J}$ are sparse matrices. Matrix $\mathcal{B}(k)$ has, at most, one nonzero entry at each row, $b_{i,2\,i}(k) = 4\,k\;b_{2\,i}$, $1 \leq i \leq J$. With respect to $\mathcal{D}(k)$, there are, at most, two nonzero entries at each row. That is, for $2 \leq i \leq 2\,J$, $d_{i,i-r_i}(k) = (1 + i\,(1 - e^{-k}) - r_i)\,e^{-k\,\mu_i^*}$ and $d_{i,i-r_i+1}(k) = (r_i - i\,(1 - e^{-k}))\,e^{-k\,\mu_i^*}$; and, $d_{1,1}(k) = e^{-k\,\mu_1^*}$, if we assume that $k < \ln(2)$. The explicit definition of the numerical method is given by means of

$$\mathbf{U}^{n+1} = \mathcal{A}(k)\,\mathbf{U}^n, \quad 0 \leq n \leq N-1,$$

where $\mathcal{A}(k) = (\mathcal{I} - \mathcal{B}(k))^{-1}\,\mathcal{D}(k)$.

Now, we suppose that u is the solution to problem (1.1)-(1.2), and we define

$$\mathbf{u}^n = (u_1^n, \ldots, u_{2\,J}^n),\;\; u_j^n = u(X_j, t^n),\;\; 1 \leq j \leq 2\,J,\;\; 0 \leq n \leq N.$$

On the one hand, the *local discretization error*, $\boldsymbol{\tau}^{n+1} = (\tau_1^{n+1}, \ldots, \tau_{2\,J}^{n+1})$, $0 \leq n \leq N-1$, is given by

$$\boldsymbol{\tau}^{n+1} = \frac{1}{k}\,\left(\mathbf{u}^{n+1} - \mathcal{A}(k)\,\mathbf{u}^n\right), \quad 0 \leq n \leq N-1. \tag{3.1}$$

On the other hand, we introduce the *global discretization error* as $\mathbf{E}^n = (E_1^n, E_2^n, \ldots, E_{2\,J}^n)$, $E_j^n = u_j^n - U_j^n$, $1 \le j \le 2\,J$, $0 \le n \le N$. Thus,

$$\mathbf{E}^{n+1} = \mathcal{A}(k)\,\mathbf{E}^n + k\,\boldsymbol{\tau}^{n+1}, \quad 0 \le n \le N.$$

From now on, C will denote a positive constant which is independent of k, for k small enough, n ($0 \le n \le N$) and j ($0 \le j \le 2\,J$); C possibly has different values in different places. We also employ the following notation, we denote by $\|\mathbf{v}\|_\infty$, the maximum norm of a vector $\mathbf{v} = (v_1, v_2, \ldots, v_{2\,J})$, and with $\|\mathcal{A}\|_\infty$ the operator maximum norm of a general matrix $\mathcal{A} = (a_{ij})_{i,j=1}^{2\,J}$, where

$$\|\mathcal{A}\|_\infty = \max_{1 \le i \le 2\,J} \left\{ \sum_{j=1}^{2\,J} |a_{ij}| \right\}.$$

The consistency analysis and the boundedness of $\|\mathcal{A}(k)\|_\infty$ will give us the convergence.

Lemma 3.1 (Stability). *Let μ^* and b be bounded on $(0, 1]$. Then*

$$\|\mathcal{A}(k)\|_\infty \le 1 + C\,k, \tag{3.2}$$

for $k > 0$ small enough.

Proof. On the one hand, as b is bounded, $\|\mathcal{B}(k)\|_\infty \le 4\,k\,\|b\|_\infty$, where we define $\|b\|_\infty = \sup_{0<x\le 1} |b(x)|$. Thus, for k small enough, $\|\mathcal{B}(k)\|_\infty < 1$. Then

$$(\mathcal{I} - \mathcal{B}(k))^{-1} = \sum_{m=0}^{\infty} \mathcal{B}(k)^m$$

and

$$\begin{aligned} \|(\mathcal{I} - \mathcal{B}(k))^{-1}\|_\infty &\le \sum_{m=0}^{\infty} \|\mathcal{B}(k)\|_\infty^m = \frac{1}{1 - \|\mathcal{B}(k)\|_\infty} \\ &\le \frac{1}{1 - 4\,k\,\|b\|_\infty} = 1 + k\,\frac{4\,\|b\|_\infty}{1 - 4\,k\,\|b\|_\infty} \\ &\le 1 + C\,k, \end{aligned} \tag{3.3}$$

for $k \le k_0$ with $4\,k_0\,\|b\|_\infty < 1$. On the other hand,

$$\begin{aligned} \|\mathcal{D}(k)\|_\infty \le \max \Big\{ & e^{-k\,\mu_1^*}, \\ & \max_{2 \le j \le 2\,J} \left\{ |1 + j\,(1 - e^{-k}) - r_j|\, e^{-k\,\mu_j^*} + |r_j - j\,(1 - e^{-k})|\, e^{-k\,\mu_j^*} \right\} \Big\}. \end{aligned} \tag{3.4}$$

We observe that conditions $X_{j-r_j} \le Y_j < X_{j-r_j+1}$, $1 \le j \le 2\,J$, are equivalent to the positivity of both expressions inside the absolute value in (3.4). Then, taking into

account the regularity of function μ^*, we arrive at

$$\|\mathcal{D}(k)\|_\infty \;\leq\; 1 + C\,k.$$

Finally, $\|\mathcal{A}(k)\|_\infty \leq \|(\mathcal{I} - \mathcal{B}(k))^{-1}\|_\infty \|\mathcal{D}(k)\|_\infty$ and we conclude with the estimate (3.2). □

Lemma 3.2 (Consistency)**.** *Let functions μ^* and b have bounded and continuous first derivative on $(0,1]$, and let u have Lipschitz continuous first derivatives in $(0,1]\times[0,T]$. Then, as $k \to 0$, assuming a constant rate $r = k/h$, the following estimates hold*

$$||\boldsymbol{\tau}^{n+1}||_\infty = O(k), \quad 0 \leq n \leq N-1. \tag{3.5}$$

Proof. The equation (3.1) allows us to write

$$\boldsymbol{\tau}^{n+1} = (\mathcal{I} - \mathcal{B}(k))^{-1}\,\frac{1}{k}\,\left((\mathcal{I} - \mathcal{B}(k))\,\mathbf{u}^{n+1} - \mathcal{D}(k)\,\mathbf{u}^n\right) = (\mathcal{I} - \mathcal{B}(k))^{-1}\,\boldsymbol{\varepsilon}^{n+1},$$

$0 \leq n \leq N-1$, where the definitions of $\mathcal{B}(k)$ and $\mathcal{D}(k)$ allow us to describe the components of the vector $\boldsymbol{\varepsilon}^{n+1}$ as

$$\varepsilon_1^{n+1} \;=\; \frac{1}{k}\left(u_1^{n+1} - u_1^n\,\exp\{-k\,\mu_1^*\} - 4\,k\,b_2\,u_2^{n+1}\right), \tag{3.6}$$

$$\varepsilon_j^{n+1} \;=\; \frac{1}{k}\left(u_j^{n+1} - \bar{u}_j^n\,\exp\left\{-k\,\mu_j^*\right\} - 4\,k\,b_{2\,j}\,u_{2\,j}^{n+1}\right), 2 \leq j \leq J, \tag{3.7}$$

$$\varepsilon_j^{n+1} \;=\; \frac{1}{k}\left(u_j^{n+1} - \bar{u}_j^n\,\exp\left\{-k\,\mu_j^*\right\}\right),\; J+1 \leq j \leq 2\,J. \tag{3.8}$$

In (3.7) and (3.8), assuming $k < \ln(2)$,

$$\bar{u}_j^n = u_{j-r_j}^n + (u_{j-r_j+1}^n - u_{j-r_j}^n)\,\frac{Y_j - X_{j-r_j}}{h},\; 2 \leq j \leq 2\,J.$$

Now, we use equation (2.3) in (3.6) to achieve,

$$\begin{aligned}\varepsilon_1^{n+1} = \frac{1}{k}\Bigg(&u(X_1\,e^{-k}, t^n)\,\exp\left\{-\int_{t^n}^{t^{n+1}}\mu^*\left(x(\tau; t^{n+1}, X_1)\right)\,d\tau\right\}\\ &+ 4\int_{t^n}^{t^{n+1}}\exp\left\{-\int_\tau^{t^{n+1}}\mu^*\left(x(s; t^{n+1}, X_1)\right)ds\right\}b(2\,x(\tau; t^{n+1}, X_1))\,u(2\,x(\tau; t^{n+1}, X_1), \tau)d\tau\\ &- \left(u_1^n\,\exp\{-k\,\mu_1^*\} + 4\,k\,b_2\,u_2^{n+1}\right)\Bigg).\end{aligned}$$

Next, we transform the equation in the following inequality

$$
\begin{aligned}
|\varepsilon_1^{n+1}| \leq \frac{1}{k}\, u(X_1\, e^{-k}, t^n) \left| \exp\left\{ -\int_{t^n}^{t^{n+1}} \mu^*\left(x(\tau; t^{n+1}, X_1)\right)\, d\tau \right\} - \exp\left(-k\, \mu_1^*\right) \right| \\
+ \frac{1}{k}\, e^{-k\,\mu_1^*} \left| u(X_1\, e^{-k}, t^n) - u_1^n \right| \\
+ \frac{4}{k} \left| \int_{t^n}^{t^{n+1}} \exp\left\{ -\int_{\tau}^{t^{n+1}} \mu^*\left(x(s; t^{n+1}, X_1)\right) ds \right\} b(2\, x(\tau; t^{n+1}, X_1))\, u(2\, x(\tau; t^{n+1}, X_1), \tau) d\tau \right. \\
\left. -k\, b_2\, u_2^{n+1} \right|,
\end{aligned}
$$

in which we use the regularity properties of μ^*, b and u, the convergence properties of the rectangular quadrature rule, and the mean value theorem to obtain

$$
|\varepsilon_1^{n+1}| \;=\; \frac{1}{k}\,\mathcal{O}(k^2) + \frac{1}{k}\,\mathcal{O}(X_1\,(e^{-k}-1)) + \frac{1}{k}\,\mathcal{O}(k^2) \quad (h \to 0,\, k \to 0).
$$

Now, the definition of X_1 allows us to arrive at

$$
\begin{aligned}
|\varepsilon_1^{n+1}| \;&=\; \frac{1}{k}\,\mathcal{O}(k^2) + \frac{1}{k}\,\mathcal{O}(h\,(e^{-k}-1)) + \frac{1}{k}\,\mathcal{O}(k^2) \quad (h \to 0,\, k \to 0) \\
&=\; \mathcal{O}(k) \quad (h \to 0,\, k \to 0).
\end{aligned} \tag{3.9}
$$

Next, we use equation (2.3) in (3.7), $2 \leq j \leq J$, to achieve

$$
\begin{aligned}
\varepsilon_j^{n+1} = \frac{1}{k} \left(u(Y_j, t^n)\, \exp\left\{ -\int_{t^n}^{t^{n+1}} \mu^*\left(x(\tau; t^{n+1}, X_j)\right)\, d\tau \right\} - \bar{u}_j^n\, \exp\left\{-k\,\mu_j^*\right\} \right) \\
+ \frac{4}{k} \left(\int_{t^n}^{t^{n+1}} \exp\left\{ -\int_{\tau}^{t^{n+1}} \mu^*\left(x(s; t^{n+1}, X_j)\right) ds \right\} b(2\, x(\tau; t^{n+1}, X_j))\, u(2\, x(\tau; t^{n+1}, X_j), \tau) d\tau \right. \\
\left. -k\, b_{2\,j}\, u_{2\,j}^{n+1} \right).
\end{aligned}
$$

Then, we transform it into the following inequation

$$
\begin{aligned}
|\varepsilon_j^{n+1}| \leq \frac{1}{k}\, u(Y_j, t^n) \left| \exp\left\{ -\int_{t^n}^{t^{n+1}} \mu^*\left(x(\tau; t^{n+1}, X_j)\right)\, d\tau \right\} - e^{-k\,\mu_j^*} \right| \\
+ \frac{1}{k}\, e^{-k\,\mu_j^*} \left| u(Y_j, t^n) - \left(u_{j-r_j}^n + (u_{j-r_j+1}^n - u_{j-r_j}^n)\, \frac{Y_j - X_{j-r_j}}{h} \right) \right| \\
+ \frac{4}{k} \left| \int_{t^n}^{t^{n+1}} \exp\left\{ -\int_{\tau}^{t^{n+1}} \mu^*\left(x(s; t^{n+1}, X_j)\right) ds \right\} b(2\, x(\tau; t^{n+1}, X_j))\, u(2\, x(\tau; t^{n+1}, X_j), \tau) d\tau \right. \\
\left. -k\, b_{2\,j}\, u_{2\,j}^{n+1} \right|,
\end{aligned}
$$

where we apply the regularity properties of μ^*, b and u, the convergence properties of rectangular quadrature rule and linear interpolation, and the mean value theorem to

arrive at

$$|\varepsilon_j^{n+1}| \leq C\, k. \tag{3.10}$$

Finally, we employ the same procedure to bound (3.8), $J+1 \leq j \leq 2\,J$, and thus,

$$|\varepsilon_j^{n+1}| \quad \leq \quad C\, k. \tag{3.11}$$

Then (3.3) and (3.9)-(3.11) produce the estimate (3.5). □

In the following result, we prove the convergence assuming that the discretization steps k, h, are chosen in such a way we keep constant the proportion $r = k/h$.

Theorem 3.3. *Under the hypotheses of Lemma 3.2, if* $\|\mathbf{E}^0\|_\infty = O(k)$, *as* $k \to 0$, *then*

$$\|\mathbf{E}^n\|_\infty = O(k), \quad 0 \leq n \leq N, \tag{3.12}$$

as $k \to 0$.

Proof. From the definition of the *global discretization error*, we have

$$\mathbf{E}^n \quad = \quad \mathcal{A}(k)\,\mathbf{E}^{n-1} + k\,\boldsymbol{\tau}^n = \mathcal{A}^n(k)\,\mathbf{E}^0 + k\,\sum_{l=0}^{n-1} \mathcal{A}^l(k)\,\boldsymbol{\tau}^{n-l}, \quad 1 \leq n \leq N.$$

Then

$$\|\mathbf{E}^n\|_\infty \quad \leq \quad (\|\mathcal{A}(k)\|_\infty)^n\ \|\mathbf{E}^0\|_\infty + k\,\sum_{l=0}^{n-1} (\|\mathcal{A}(k)\|_\infty)^l\ \|\boldsymbol{\tau}^{n-l}\|_\infty, \quad 1 \leq n \leq N.$$

Therefore, the use of (3.2), (3.5) and $k = r\,h$, produces (3.12]. □

4. Numerical experiments

As a first experiment to evaluate the unconditional stability and the optimal rate of convergence of the method, we consider the case when $\mu(x) = \nu(x)$. This situation models a cell population in which the dynamics is only driven by the division rate of the individuals. We take the size-specific division rate function as

$$b(x) = 2^6\, x^3\ (1-x)^3\,, \qquad 0 < x \leq 1,$$

and the initial data,

$$\varphi(x) = \varphi_c \cdot (1-x)\, x^3\ (\sin(\pi\,(4\,x+1)) + 1)\,, \qquad 0 < x \leq 1,$$

where φ_c is the chosen constant to obtain $\max_{0<x\leq 1}(\varphi(x)) = 1$. This model problem was also considered by Abia *et al.* [2] for testing the upwind scheme and a first-order natural grid method. In contrast with those methods, the semi-Lagrangian approach we consider here produces an unconditionally stable scheme.

We compute the numerical solution until a final time $T = 1$ for different values of the discretization parameters. As we do not know an analytical expression for the exact solution of this problem, the global discretization errors are computed by comparing the numerical solution $\mathbf{U}^n_{k,h}$, $0 \leq n \leq N$, with a fixed approximation to the exact solution, $\mathbf{U}^{n^*}_{k^*,h^*}$, $0 \leq n^* \leq N^*$, calculated with very small values for the size and time steps (in this case, we take $h^* = k^* = 1.525886 \cdot 10^{-5}$). To make comparisons possible, both the discretization size and time steps, h^* and k^*, are chosen as an appropriate division by a power of two of the coarsest values of h and k in the numerical experiments.

Then, for each h and k, we compare at every time step $t^n = n\,k$, $0 \leq n \leq N$, the numerical approximations $(U^n_{k,h})_j$, $0 \leq n \leq N$, $0 \leq j \leq 2\,J$, with the corresponding nodal approximations $(U^{n^*}_{k^*,h^*})_{j^*}$, $0 \leq n^* \leq N^*$, $0 \leq j^* \leq 2\,J^*$, $j\,h = j^*\,h^*$, $n\,k = n^*\,k^*$, of the computed exact solution, and we define

$$e_{k,h} = \max_{0\leq n\leq N} \max_{0\leq j\leq 2J} |(U^n_{k,h})_j - (U^{n^*}_{k^*,h^*})_{j^*}|. \tag{4.1}$$

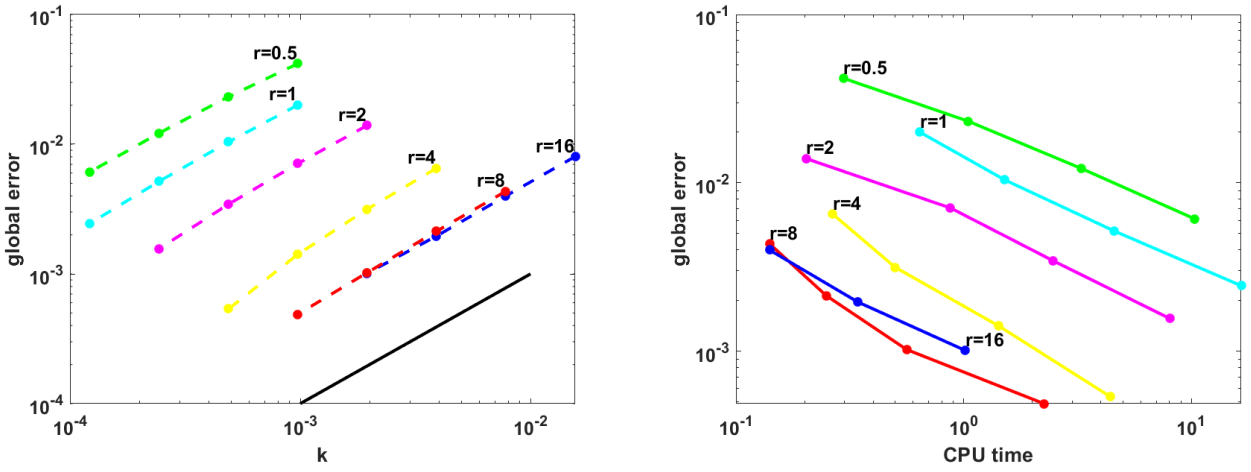

Figure 1. On the left: global error plots obtained with the numerical scheme with different values of r (dashed lines). Solid line shows order 1. On the right: efficiency plot of the semi-Lagrangian method with different values of r.

In Figure 1, we represent efficiency plots using logarithm scales for both axes: global error versus time discretization parameter, on the left, and global error versus CPU time, on the right. In both, the global error is computed with formula (4.1). Each dot on the left plot corresponds to the discretization for given values of the parameters h and k: from the coarsest value of k taken equal to $1.562 \cdot 10^{-2}$ with $r = 16$, to the finest value of k equal to $1.220 \cdot 10^{-4}$ with $r = 0.5$. The first order of convergence is clearly confirmed by the slope of each curve of global error versus k for constant $r = k/h$ (here we clearly observe the first-order convergence which is represented by a solid line). The most efficient implementation of the method corresponds to a relationship between the time and size parameters of $r = 8$.

Figure 2 presents a comparison of the efficiency plots (global error versus CPU time) of the proposed numerical scheme with the upwind and the natural grid methods

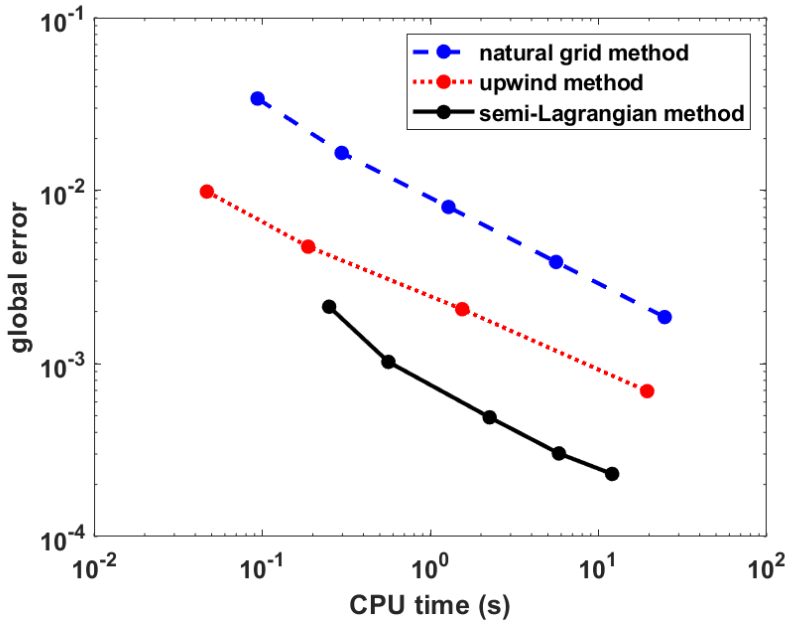

Figure 2. Efficiency plot (global error vs. CPU time): comparison of the efficiency of natural grid method (blue dashed line), upwind method (red dotted line) and semi-Lagrangian method, $r = 8$ (black solid line).

studied in [2]. We show how the semi-Lagrangian method is the most efficient.

We also want to pay attention to the behavior of the numerical method when dealing with singularities of the solution. For constant division rate functions, the discontinuity of the division rate function at $x = 1$ produces discontinuities of the first and second derivatives of the solution at sizes $x = 1/2$ and $x = 1/4$, respectively. This lack of smoothness of the solution was not considered in the convergence theorems of the previous section. However, we illustrate the numerical resolution of these discontinuities with the analyzed numerical method. With this purpose, we have performed a numerical experiment on the model with constant biological rate functions $b(x) = 4$, $\mu(x) = 4$, and $\nu(x) = 0$, in $[0, 1]$. In this case, at $T = 1$, we observe that the approximated first derivative of u is discontinuous at $x = 0.5$ but it is continuous at $x = 0.25$ (Figure 3, first row) and the approximated second derivative of u is discontinuous both at $x = 0.25$ and $x = 0.5$ (Figure 3, second row).

In the case of constant rate functions, we can compute the theoretical solution of the model problem (1.1)-(1.2) by means of the formula (1.3). For example, in Figure 4 we present the solution, at $T = 1$, when $b(x) = 0.5$, $\mu(x) = 0.5$ and $\nu(x) = 0$ (left plot), and $b(x) = 2$, $\mu(x) = 2$ and $\nu(x) = 0$ (right plot). We have observed that, as we increase the constant division rate, the theoretical solution $u(x, t)$ shows strong oscillations with increasing amplitudes and frequencies, close to the boundary $x = 0$, making the approximation to the solution even more difficult. This is reflected in the loss of the convergence order we get for the numerical solution when, for example, $b(x) = 2$, $\mu(x) = 2$, and $b(x) = 4$, $\mu(x) = 4$.

However, the numerical solution computed with the analyzed numerical scheme (2.4)-(2.5), with discretization parameters $k = h = 6.1035 \cdot 10^{-5}$, reproduce the same theoretical solution given by (1.3). This behavior involves the growth of the cell population with small sizes as the constant division rate increases. It is convenient

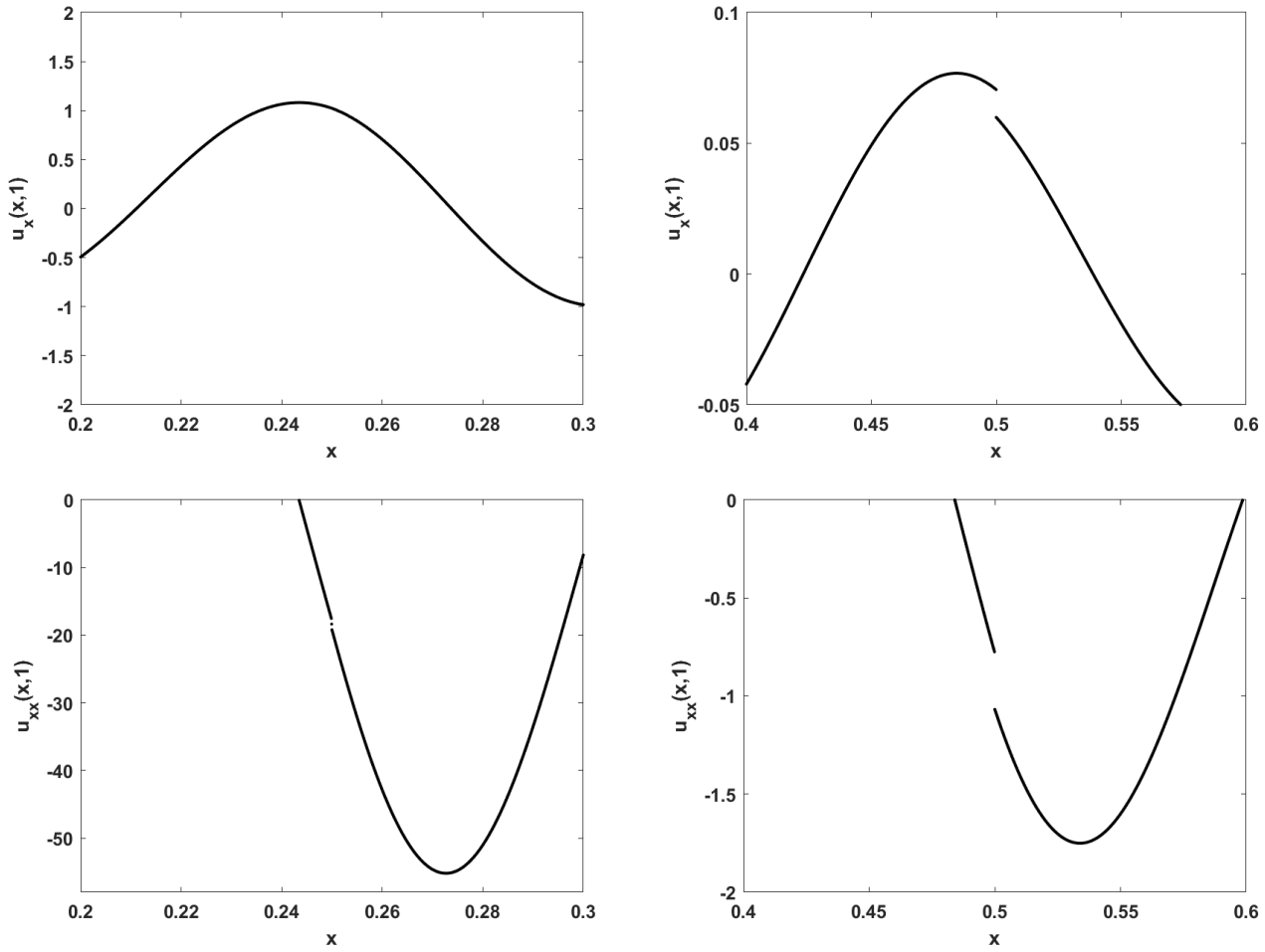

Figure 3. Approximated first (first row) and second derivative (second row) of u around $x = 0.25$ and $x = 0.5$ at $T = 1$.

to know what its impact is on the whole cell population, which is measured through the proportion of *dwarf* cells in the population. With this goal, we fix a threshold $x = x_\alpha > 0$, and we compute the values

$$\alpha(t) = \frac{\displaystyle\int_0^{x_\alpha} u(x,t)\,dx}{\displaystyle\int_0^{1} u(x,t)\,dx}, \quad 0 \le t \le T. \tag{4.2}$$

The quantity $\alpha(t)$ represents the time evolution of a measure of the proportion of dwarf cells (cells with size less than the threshold value $x_\alpha > 0$) within the total proliferating cell population. Figure 5 shows the curves we obtain for constant values of b in the range $0 \le b \le 1$, for the time interval $[0, 50]$ and a threshold value $x_\alpha = 0.125$. It shows how this proportion is increasing to one, which represents a mathematical predictor of a size distribution disorder in the population.

Finally, we declare that the whole computation was carried out using double precision arithmetic on a personal computer with an Intel i7-4790 CPU.

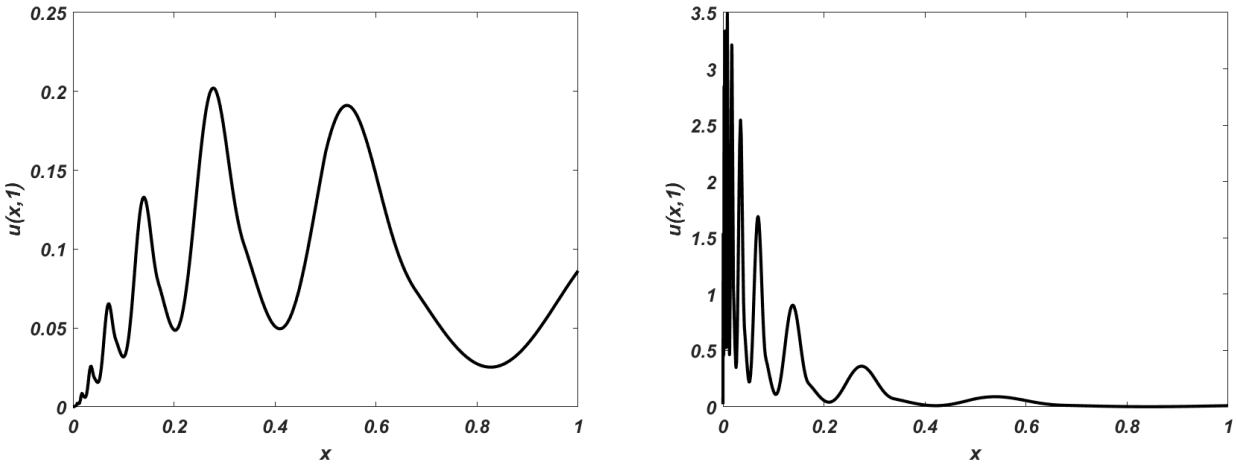

Figure 4. Solution values computed with the theoretical solution with different constant vital functions. Plot on the left: $b(x) = 0.5$, $\mu(x) = 0.5$. Plot on the right: $b(x) = 2$, $\mu(x) = 2$.

5. Conclusions

The study of cell populations by means of structured population models, and their numerical simulation, are current topics of interest. In this work we have proposed a new numerical method to attain the solution to a size-structured population model describing the dynamics of a cell population when the reproduction process is achieved by division into two equal parts in a particular situation. This specific problem allows the division of cells of all sizes, a modeling aproach to describe the phenomenom of "dwarfism", appearing as a dynamic size-distribution disorder in certain blood diseases.

We have designed a semi-Lagrangian numerical scheme based on the integration along the characteristic curves using a fixed uniform grid on the size of cells interval. Therefore, the size grid is not recomputed at each time step. With this approach, the resulting numerical method is unconditionally stable, in contrast with numerical methods based on finite difference discretizations of the problem. We have proved first-order convergence for smooth solutions, and we have corroborated this behavior experimentally.

From a biological point of view, we have shown, via simulations, how the increase of the division rate of small size cells promotes a dynamics in which nonfunctional dwarf cells are saturating the total cell population.

We have also presented the size behavior of the proposed numerical scheme in stressed situations in which solutions present discontinuities in the first and second derivatives.

Funding

This research was funded in part by project MTM2017-85476-C2-1-P of the Spanish Ministerio de Economía y Competitividad, and European FEDER Funds, grant PID2020-113554GB-I00/AEI/10.13039/501100011033 grant RED2018-102650-T funded by MCIN/AEI/10.13039/501100011033, and research grant VA193P20 of

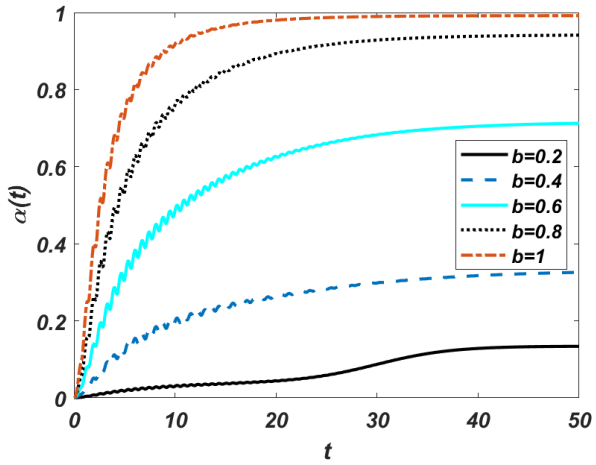

Figure 5. Proportion of dwarf cells ($\alpha(t)$), computed with (4.2) with $t \in [0, 50]$.

the Junta de Castilla y León, Spain, and European FEDER funds (EU).

Acknowledgements

The authors are very grateful to the anonymous referees for his/her careful reading of the original manuscript and his/her aid to improve it.

References

[1] L. M. Abia, O. Angulo, J. C. López-Marcos, and M. A. López-Marcos, Numerical schemes for a size-structured cell population model with equal fission. Math. Comp. Model. 50 (2009), pp. 653–664.

[2] L. M. Abia, O. Angulo, J. C. López-Marcos, and M. A. López-Marcos, Numerical analysis of a cell dwarfism model. J. Comp. App. Math. 349 (2019), pp. 82-92

[3] O. Angulo, J. C. López-Marcos, and M. A. López-Marcos, A semi-Lagrangian method for a cell population model in a dynamical environment. Math. Comp. Model. 57 (2013), pp. 1860–1866.

[4] O. Angulo, J. C. López-Marcos, and M. A. López-Marcos, A second-order method for the numerical integration of a size-structured cell population model. Abstr. Appl. Anal. (2015), 549168, pp. 1-8,

[5] O. Angulo, J. C. López-Marcos, and M. A. López-Marcos, A second-order numerical method for a cell population model with asymmetric division. J. Comp. Appl. Math. 309 (2017), pp. 522–531.

[6] O. Diekmann, H. J. A. M. Heijmans, and H. R. Thieme, On the stability of the cell size distribution. J. Math. Biol. 19 (1984), pp. 227–248.

[7] R. Galanello, and A. Cao, α-thalassemia. Genetics in Medicine, 13 (2011), pp. 83–88.

[8] G. Geiner, and R. Nagel, Growth of cell populations via one parameter semigroups of positive operators, in Mathematical Applied to Science, J. Goldstein, S. Rosencrans, G. Sod (eds), Academic Press, London, 1988, pp. 79–104.

[9] H. J. A. M. Heijmans, On the stable size distribution of populations reproducing by fission into two unequal parts. Math. Biosci. 12 (1984), pp. 119-150.

[10] K. H. Howard, A size-structured model of cell dwarfism. Disc. Cont. Dyn. Sys. B 1 (2001), pp. 471-484.
[11] S. El Mourchid, G. Metafuneb, A. Rhandi, and J. Voigt, On the chaotic behaviour of size structured cell populations. J. Math. Anal. Appl. 339 (2008), pp. 918–924.
[12] R. Rudnicki, Chaoticity and invariant measures for a cell population model. J. Math. Anal. Appl. 393 (2012), pp. 151–165.
[13] D. P. Steensma, R. J. Gibbons, and D. R. Higgs, Acquired α-thalassemia in association with myelodysplastic syndrome and other hematologic malignancies. Blood 105 (2005), pp. 443-452.

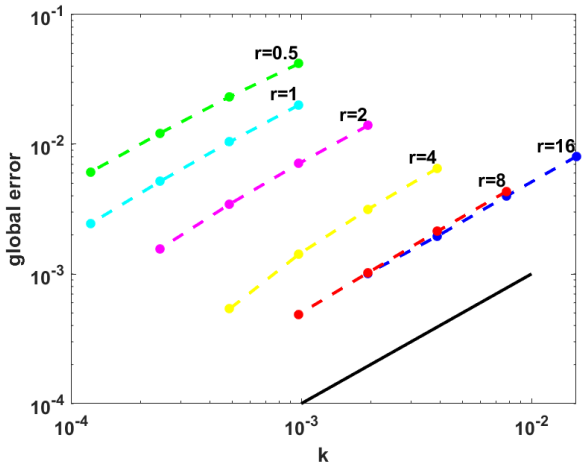
global error
k
r=0.5
r=1
r=2
r=4
r=8
r=16

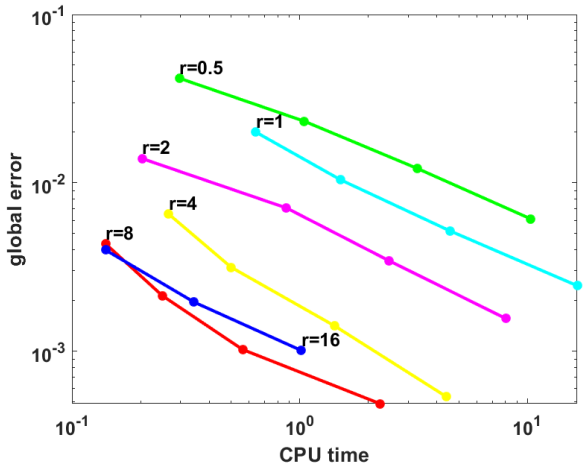
global error
CPU time
r=0.5
r=1
r=2
r=4
r=8
r=16

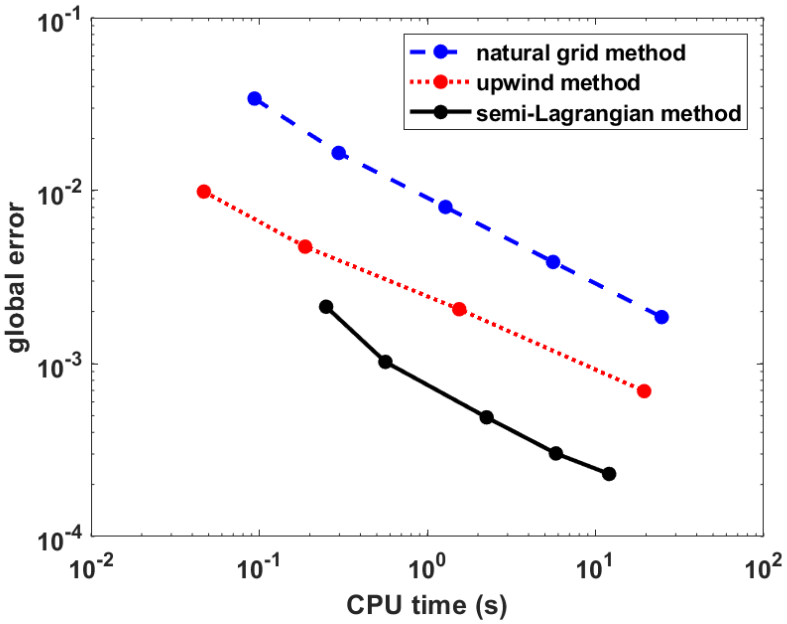
natural grid method
upwind method
semi-Lagrangian method
global error
CPU time (s)
10^-1
10^-2
10^-3
10^-4
10^-2
10^-1
10^0
10^1
10^2

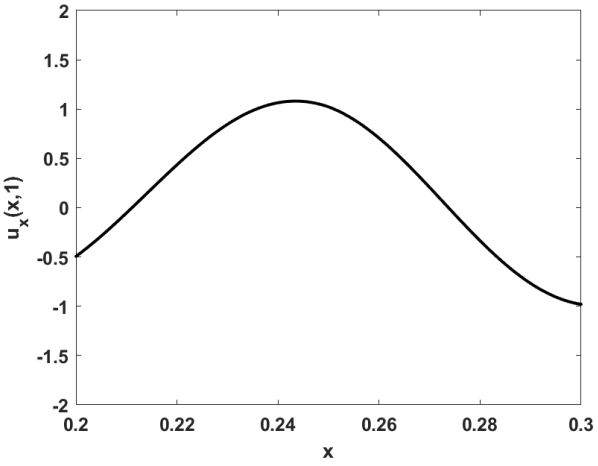
2
1.5
1
0.5
0
-0.5
-1
-1.5
-2
0.2
0.22
0.24
0.26
0.28
0.3
x
u_x(x,1)

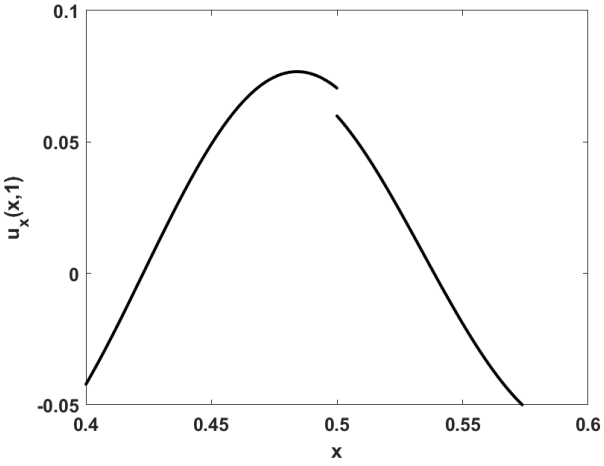
0.1
0.05
0
-0.05
0.4
0.45
0.5
0.55
0.6
x
u_x(x,1)

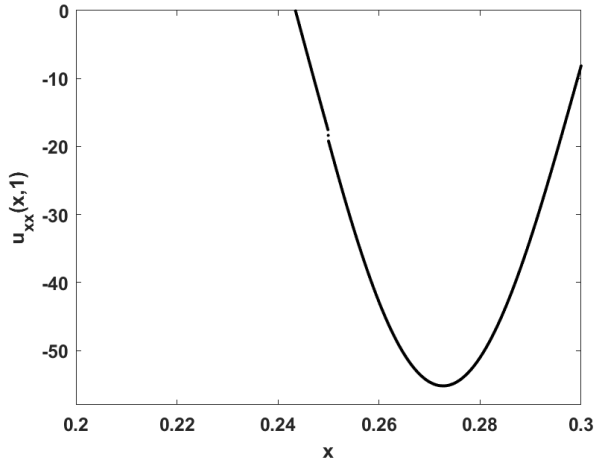
0
-10
-20
-30
-40
-50
0.2
0.22
0.24
0.26
0.28
0.3
x
u_xx(x,1)

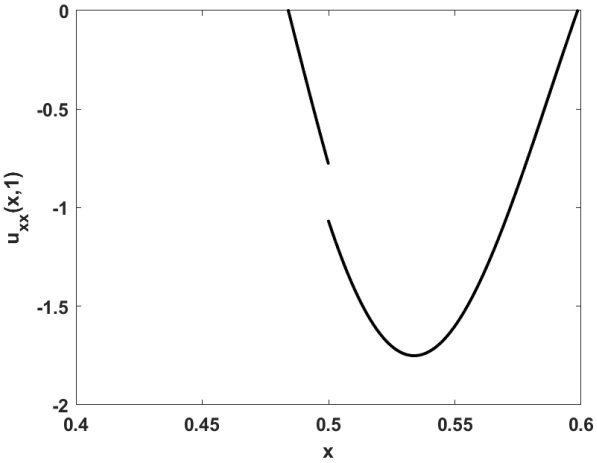
0
-0.5
-1
-1.5
-2
0.4
0.45
0.5
0.55
0.6
x
u_xx(x,1)

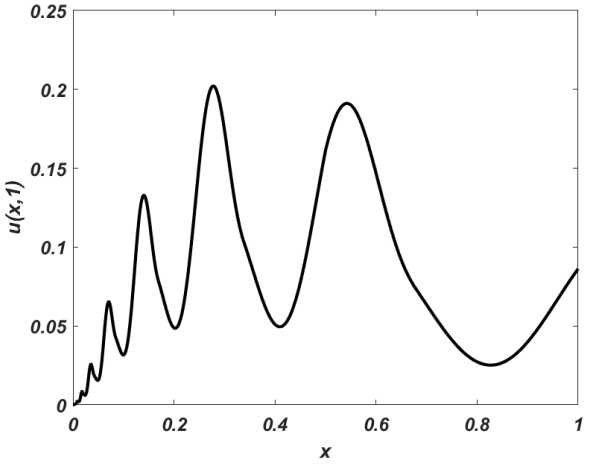
0.25
0.2
0.15
0.1
0.05
0
u(x,1)
0
0.2
0.4
0.6
0.8
1
x

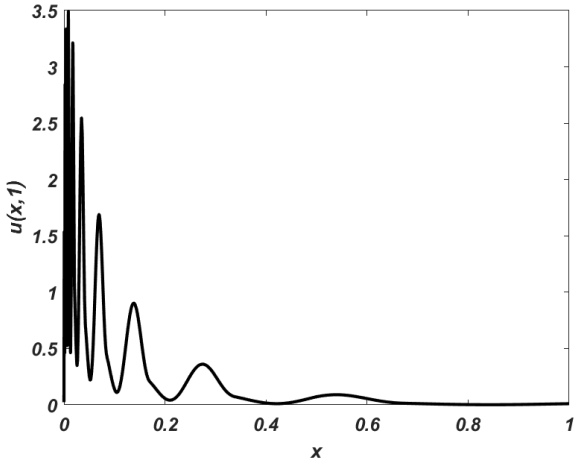
3.5
3
2.5
2
1.5
1
0.5
0
u(x,1)
0
0.2
0.4
0.6
0.8
1
x

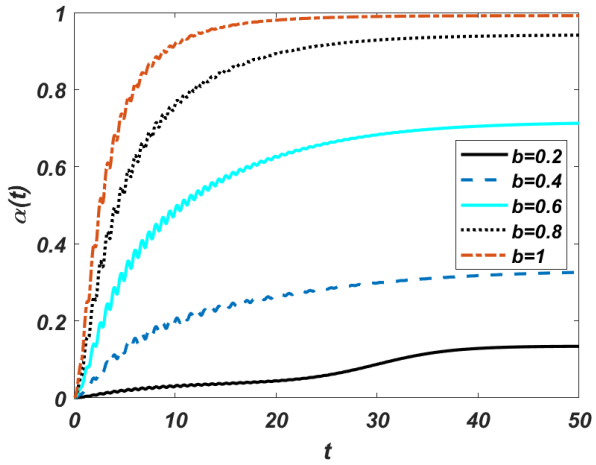
1
0.8
0.6
0.4
0.2
0
α(t)
0
10
20
30
40
50
t
b=0.2
b=0.4
b=0.6
b=0.8
b=1

Captions of Figures

- Figure 1: On the left: global error plots obtained with the numerical scheme with different values of r (dashed lines). Solid line shows order 1. On the right: efficiency plot of the semi-Lagrangian method with different values of r.
- Figure 2: Efficiency plot (global error vs. CPU time): comparison of the efficiency of natural grid method (blue dashed line), upwind method (red dotted line) and semi-Lagrangian method, $r = 8$ (black solid line).
- Figure 3: Approximated first (first row) and second derivative (second row) of u around $x = 0.25$ and $x = 0.5$ at $T = 1$.
- Figure 4: Solution values computed with the theoretical solution with different constant vital functions. Plot on the left: $b(x) = 0.5$, $\mu(x) = 0.5$. Plot on the right: $b(x) = 2$, $\mu(x) = 2$.
- Figure 5: Proportion of dwarf cells ($\alpha(t)$), computed with (4.2) with $t \in [0, 50]$.